Technical Annals

Vol 1, No 5 (2024)

Technical Annals

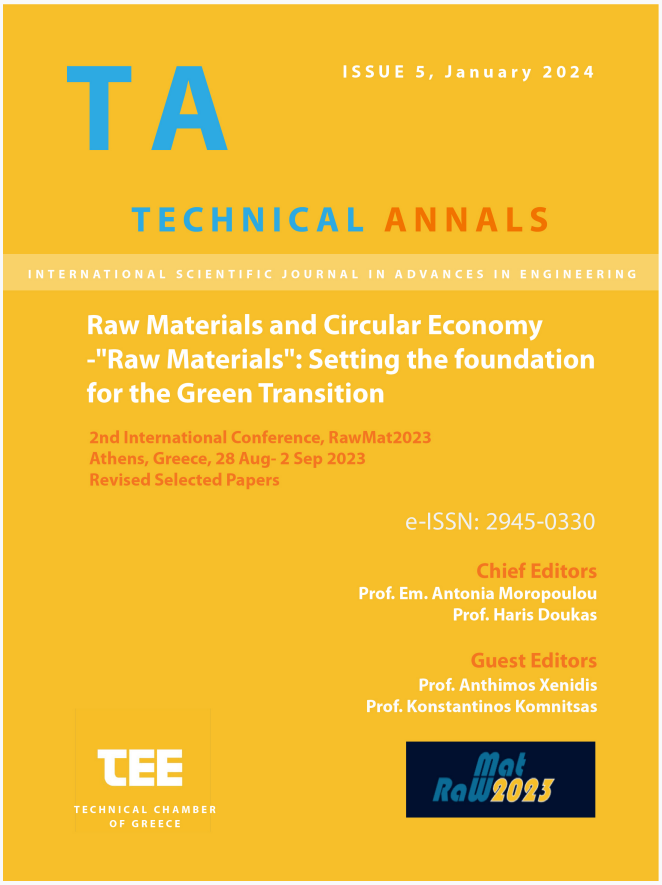

Hydrometallurgical recovery of EoL LFP batteries using oxalic acid as leaching agent

Rafaella-Aikaterini Megaloudi, Anthimos Xenidis, Nikolaos Konsolas, Paschalis Oustadakis

doi: 10.12681/ta.41680

To cite this article:

Megaloudi, R.-A., Xenidis, A., Konsolas, N., & Oustadakis, P. (2024). Hydrometallurgical recovery of EoL LFP batteries using oxalic acid as leaching agent. *Technical Annals*, *1*(5). https://doi.org/10.12681/ta.41680

Hydrometallurgical recovery of EoL LFP batteries using oxalic acid as leaching agent

Rafaella-Aikaterini Megaloudi, Nikolaos Konsolas, Paschalis Oustadakis, Anthimos Xenidis

School of Mining and Metallurgical Engineering, National Technical University of Athens 9, Iroon Polytechniou st., 15780 Athens, Greece
axen@metal.ntua.gr

Abstract. The extraction of lithium (Li), iron (Fe), aluminum (Al), and copper (Cu) by oxalic acid solution from lithium iron phosphate (LFP) electric vehicle batteries was systematically investigated. Following battery disassembly, a comprehensive pretreatment scheme was employed, comprising shredding, crushing/grinding, sieving, and washing to reduce particle size and recover valuable battery materials in a stream collectively known as black mass. The black mass primarily contains the valuable components of the anode (graphite) and cathode ($LiFePO_4$), as well as impurities such as aluminum and copper foils used as current collectors. Leaching experiments were conducted by varying oxalic acid concentration, temperature, and leaching time. Lithium extraction reached 100% at an oxalic acid concentration of 0.7 M, a leaching temperature of 70 °C, a liquid-to-solid ratio of 10 l/kg, and a leaching time of 30 minutes. Under these conditions, iron from $LiFePO_4$ is initially dissolved but subsequently precipitated as iron oxalate and iron phosphate oxide, thereby limiting its overall extraction to very low levels (<5%). Nearly 100% of aluminum is dissolved, whereas copper dissolution remains relatively low (<2%). At lower oxalic acid concentrations, the extraction efficiencies of lithium and aluminum decrease, while remaining largely unaffected by temperature variations. Overall, the oxalic acid-based process demonstrates high efficiency for lithium extraction, effective separation from the solid matrix, and strong potential for subsequent lithium recovery from the leachate.

Keywords: LFP batteries, Li-ion batteries, leaching, oxalic acid

1 Introduction

Most of today's electric vehicles use lithium-ion batteries. To reduce costs, lithium iron phosphate ($LiFePO_4$) batteries are being considered as a more economical alternative. These batteries use cheaper electrode materials compared to other batteries in the same category and they are more reliable than the widely used NMC batteries (lithium, nickel, manganese, cobalt) [1].

The increasing demand for lithium batteries and their widespread use makes their recycling imperative. The recycling of Li-ion batteries can be summarized in three

different approaches: direct recycling, pyrometallurgy and hydrometallurgy [2]. Direct recycling presents limitations, especially regarding the continuous changes in the composition of the batteries [3]. Pyrometallurgy lacks due to the high energy consumption and strict environmental regulations that need to be followed [4]. On the other hand, hydrometallurgical methods are safer, with low energy consumption and sufficient metal recovery rates.

The hydrometallurgical processing of lithium-ion batteries has been extensively researched using both inorganic and organic acids. Inorganic acids such as HCl [5], HNO_3 [6,7], and H_2SO_4 [8], as well as organic acids such as citric acid [9,10], acetic acid [11,12], ascorbic acid [13], maleic acid [12], trichloroacetic acid and oxalic acid [14], with or without the simultaneous use of reducing agents [15], have been proposed or applied as leaching agents for lithium-ion batteries.

In this study, a hydrometallurgical method to recover Li from spent LFP batteries' cathodes involving pretreatment and leaching stages using oxalic acid as a leaching agent without the necessity of using an oxidizing agent or prior chemical or thermal pretreatment has been examined. The kinetics of the leaching and the impact of initial oxalic acid concentration and reaction temperature on the lithium, iron, aluminum and copper extraction were investigated.

2 Materials and Methods

2.1 Batteries pretreatment

A total of twelve cylindrical LFP battery cells, at the end of their lifecycle, were used in this study. These cells were collected by Bauer Energy, a Greek company specializing in the trade of small electric vehicles, primarily the Chinese BEEV cars. The batteries were fully discharged under the supervision of the company. Each battery cell weighs 144.61 g, including its plastic and metal casing.

Before proceeding with leaching experiments for element recovery from the active battery material, a detailed pretreatment process, illustrated in Fig. 1, was applied. Initially, the batteries were shredded using a shredder equipped with 15 mm-diameter blades. Then, after manual separation of the metal casing, plastic components, and paper, the material underwent further size reduction using a Pulverizer Mill LM2 by Labtechnics, followed by dry sieving, resulting in four particle size fractions: +5.6 mm, +1 mm, +0.5 mm, and -0.5 mm shown in Fig. 1.

These four fractions were processed separately to minimize the formation of metallic fines, thereby reducing their concentration in the final working sample. The -0.5 mm fraction was not further processed and constituted a part of the working sample, along with material derived from the other three fractions, as detailed in the following paragraphs.

After the first grinding, a second grinding stage of the +1 mm and +0.5 mm fractions was performed using the same equipment, followed by sieving with a 0.5 mm sieve to release and separate fine anodic or cathodic material attached to metals and plastics. Dry magnetic separation was also applied to the +5.6 mm particle size fraction, aiming to remove any magnetic material present in the sample.

The three coarse fractions obtained from the three primary and secondary sieving processes were mixed and placed in water at a liquid to solid ratio 100 l/kg to separate plastics. Then, the pulp containing the heavy fraction was further sieved using 0.5 mm sieves to remove residual coarse (+0.5 mm) material attributed to metals, paper or residual heavy plastics. The slurry thus obtained containing the fine (-0.5 mm) fraction was further filtered. The liquid from filtration was collected and the solids were placed in an oven for drying at 100°C for 48 hours. The four fine fractions (-0.5 mm) obtained from both the primary and secondary sieving were then mixed to obtain the final working sample, as illustrated in Fig. 1.

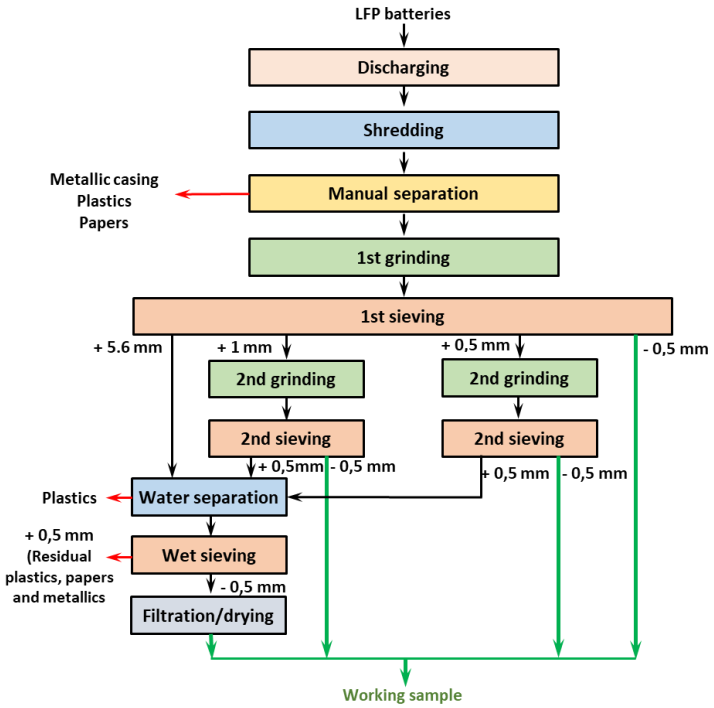

Fig. 1. LFP batteries pretreatment scheme

(a) (b) (c)

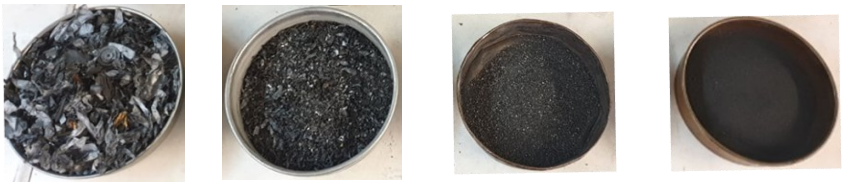

(d) (e) (f) (g)

Fig. 2. LFP batteries samples: (a) initial shredded sample (b) metallic casing, (c) material after metallics removal, (d)-(g) 1st sieving fractions ((d) +5.6mm, (e) -5.6 + 1 mm, (f) -1 + 0.5mm, (g) -0.5 mm)

2.2 Sample characterization

Chemical analysis of the working sample was conducted by fusion with borax of a finely ground subsample to a particle size of <75 μm, involving mixing of 0.1 g of the working sample with 1.5 g of a mixture of analytical grade potassium carbonate, sodium carbonate, and sodium tetraborate decahydrate at a molar ratio of 1:1:1. The mixture was then heated in a platinum crucible at 1000°C for 1 hour. The fused bead was transferred to a PTFE beaker, and an appropriate volume of diluted mineral acid (HCl) was added. The mixture was gently heated at 60–80°C under continuous stirring until fully dissolved. The resulting solution was diluted to a known volume with deionized water and analyzed by ICP-OES (Optima 7000, PerkinElmer, Akron, OH, USA) and atomic absorption spectroscopy (AAS) (PinAAcle 900T, PerkinElmer, Akron, OH, USA).

Mineralogical analysis was performed by X-ray diffraction analysis (XRD, D8 Focus, Bruker, Billerica, MA, USA) and scanning electron microscopy (SEM) using a Jeol 6380LV (JEOL Ltd., Tendo-shi, Japan).

2.3 Leaching experiments

A borosilicate round-bottom glass reactor with a total volume of 0.5 L, fitted with a five-port cap to accommodate various operational requirements, was used for the leaching experiments. The reactor was equipped with a thermomantle to ensure uniform heating and precise temperature control at 50, 70, or 90 °C. To mitigate excessive foaming observed during the reaction between the black mass and oxalic acid dihydrate ($C_2H_2O_4 \cdot 2H_2O$, >99%, Sigma-Aldrich), the reactor was loaded with only 300 mL of oxalic acid solution.

Leaching experiments were performed using oxalic acid solutions at concentrations of 0.1, 0.2, 0.5, and 0.7 M, with a fixed liquid-to-solid (L/S) ratio of 10 l/kg. Each experiment was conducted for 120 minutes under continuous stirring at 500 rpm. During the leaching process, four 5 mL aliquots were collected at 15, 30, 60, and 80 minutes. All samples, including the final bulk solution at the end of the experiment, were filtered, and the resulting filtrates were analyzed using atomic absorption spectroscopy (AAS) or inductively coupled plasma optical emission spectroscopy (ICP-OES). The pH of the final leachate was also measured. Solid residues were dried at

100 °C, weighed, and characterized by X-ray diffraction (XRD) and scanning electron microscopy (SEM).

Two experimental series were systematically conducted to investigate the effects of (i) oxalic acid concentration in the leaching solution and (ii) reaction temperature, on metals extraction under constant liquid-to-solid ratio of 10 l/kg, agitation speed of 500 rpm, and a residence time of up to 120 minutes, as summarized in the table below.

Table 1. Leaching conditions

Oxalic acid conc. (M)	Volume (ml)	Temperature (°C)	Pulp density (ml/g)	Time (min)
0.1	300	70	10	120
0.2	300	70	10	120
0.5	300	70	10	120
0.7	300	70	10	120
0.5	300	50	10	120
0.5	300	70	10	120
0.5	300	90	10	120

3 Results and Discussion

3.1 Mechanical Pretreatment

Table 1 presents the mass distribution of four particle size fractions obtained from twelve lithium-ion battery cells following shredding, removal of metal casings, plastic components, and separators, and subsequent sieving.

Table 2. Particle size fractions mass after the first crushing and sieving

Particle size	Weight (g)	Percentage (%)	Black mass (g)	Percentage (%)
+ 5.6 mm	244.04	26.6	10.55	1.69
-5.6 + 1 mm	104.04	11.3	65.20	10.45
-1 + 0.5 mm	82.54	9.0	61.20	9.80
-0.5 mm	487.26	53.1	487.26	78.06
Total	**917.88**	**100.0**	**624.21**	**100.00**

As shown in Table 2, 53% of the material obtained from the initial grinding process consists of particles smaller than 0.5 mm, which are classified as black mass, primarily composed of anodic and cathodic active materials. In addition, magnetic separation of the coarse fraction (>5.6 mm) revealed that 15.9% of this fraction is magnetic, representing 4.2% of the total mass of shredded batteries after the manual removal of metallic casings.

Following the treatment scheme outlined in Fig. 1, a total of 624.21 g of black mass was recovered, representing 68% of the battery mass after manual removal of metallic casings. This black mass served as the final working sample for subsequent leaching experiments with oxalic acid. The majority (78.06%) originated from the <0.5 mm fraction obtained during the first-stage screening, while the intermediate fractions (0.5–1 mm and 1–5.6 mm) contributed 9.80% and 10.45%, respectively. Only 1.69% of the black mass was recovered from the coarse fraction (>5.6 mm).

3.2 Sample Characterization

Chemical analysis of the working black mass sample is given in Table 3.

Table 3. Chemical analysis of the LFP batteries black mass

Element	Weight (g/100g)	Atomic (moles/100g)
Li	1.90	0.274
Al	4.66	0.173
Fe	15.26	0.273
Cu	6.82	0.107
PO_4^{3-}	25.80	0.272

As shown in Table 3, the molar ratio of Li:Fe:PO_4 is 1:1:1, consistent with the stoichiometry of $LiFePO_4$. The Al and Cu contents were 4.66% and 6.82%, respectively. The loss on ignition (LOI), determined after heating at 1000 °C for one hour, was 29.39%.

The X-ray diffraction (XRD) pattern is presented in Fig. 3. The primary crystalline phases identified were triphylite ($LiFePO_4$), graphite, and metallic copper.

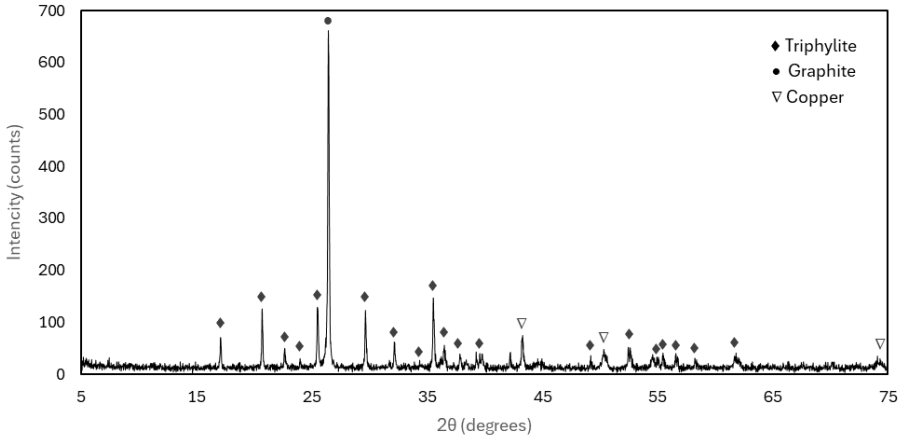

Fig. 3. XRD pattern of the working sample

The results of the SEM/EDS are shown in Fig. 4a-c. As seen in this figure, black mass consists of fine particles, approximately 25μm in size, as well as larger particles

with sizes around 500µm. Microanalyses conducted revealed the presence of $LiFePO_4$ in various particle sizes, as well as metallic elements such as copper, typically found in larger particles and aluminum (Fig. 3c).

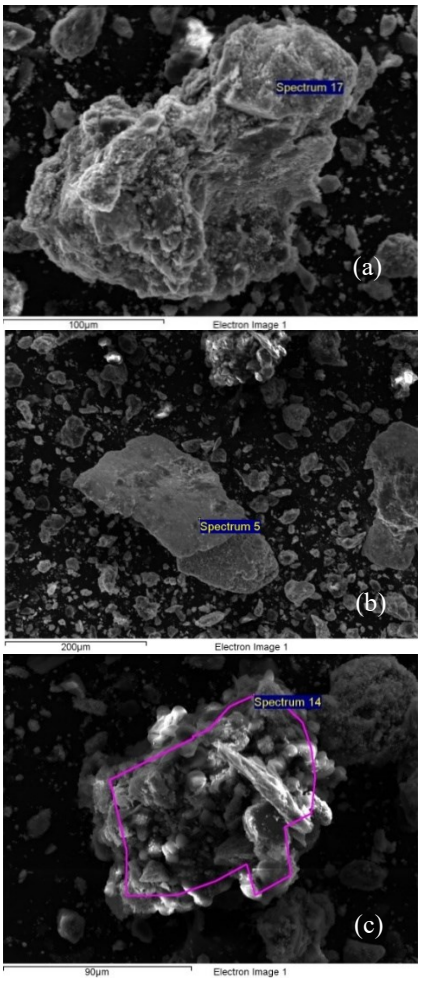

Element	Weight (%)	Atomic (%)
O	34.41	58.01
P	26.61	23.17
Fe	38.98	18.82
Totals	100.00	

Element	Weight (%)	Atomic (%)
O	1.74	6.52
Cl	0.90	1.52
Cu	97.36	91.96
Totals	100.00	

Element	Weight (%)	Atomic (%)
O	41.78	61.53
Al	21.66	18.91
P	12.21	9.29
Fe	24.35	10.27
Totals	100.00	

Fig. 4. SEM images and EDS results of the working sample (a): $LiFePO_4$, (b) metallic Cu, (c) aggregation of $LiFePO_4$ and metallic Al

3.3 Leaching tests

During black mass leaching, $LiFePO_4$ dissolves in oxalic acid solutions with lithium remaining in the solution as lithium ions whereas Fe(II) of $LiFePO_4$ will not oxidize and precipitate in the presence of oxalates to produce FeC_2O_4. The simplified reaction of $LiFePO_4$ leaching with oxalic acid is:

$$LiFePO_{4(s)} + H_2C_2O_{4(aq)} \rightarrow Li^+_{(aq)} + FeC_2O_{4(s)} + PO_4^{3-} + 2H^+$$

Change of pH and redox potential. The results of pH and redox potential of the final leaching solution as a function of initial oxalic acid concentration are presented in Fig. 5.

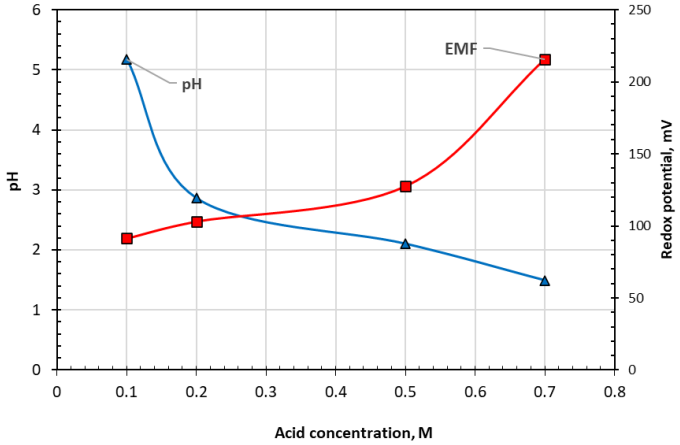

Fig. 5. Variation of final pH and redox potential as a function of oxalic acid concentration (time 120min, T=70°C , L/S 10 l/kg)

As shown in Fig. 5, the final pH of the leachate decreases with increasing oxalic acid concentration, while the redox potential increases correspondingly. Variation in temperature had no significant effect on the final pH of the leaching solution.

Effect of oxalic acid concentration. The influence of initial oxalic acid concentration and leaching time on the extraction efficiencies of Li, Fe, Cu, and Al is illustrated in Fig. 6–9. As shown in Fig. 6, complete Li extraction (100%) was achieved at an initial oxalic acid concentration of 0.7 M. At 0.5 M, Li extraction decreased to approximately 73–80%, while at 0.2 M it further declined to 30–35%. At the lowest tested concentration (0.10 M), lithium extraction was limited to around 20%.

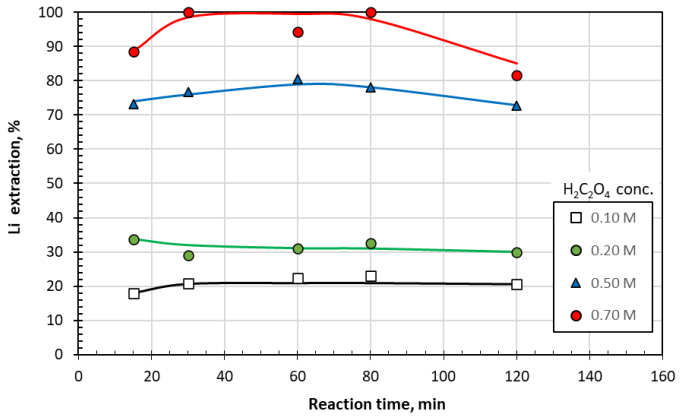

Fig. 6. Li extraction as a function of time and oxalic acid concentration (T=70°C)

In contrast, iron dissolution remained consistently low, lower than 5%, across all tested conditions and did not follow the same trend as Li (Fig 7). This behavior indicates the selective dissolution of $LiFePO_4$, likely accompanied by the reprecipitation of iron as solid iron oxalate as confirmed by the XRD patterns of the leaching residue to be presented in the following paragraphs.

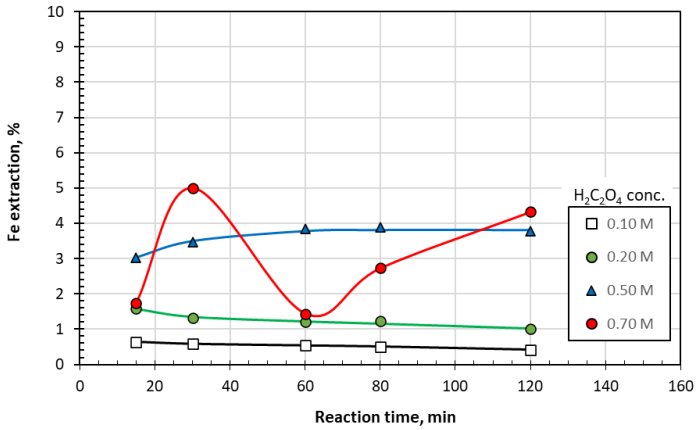

Fig. 7. Fe extraction as a function of time and acid concentration (T=70°C)

Consequently, oxalic acid serves a dual function by providing the necessary acidity for the dissolution of $LiFePO_4$ and simultaneously by supplying oxalate ions that act as ligands, promoting the precipitation of iron as iron oxalate. The highest Li extraction efficiency was observed at an oxalic acid concentration of 0.7 M. However, the iron extraction profile over time at this concentration exhibited irregularities, suggesting that time-dependent dissolution and reprecipitation processes are occurring.

Copper extraction was minimal, with concentrations in the pregnant leach solution approaching the analytical detection limits under most conditions. An exception was observed at an oxalic acid concentration of 0.7 M, where copper recovery reached approximately 10% after 120 minutes of leaching, exhibiting an increasing trend (Fig. 8).

In contrast, aluminum exhibited high leachability, achieving extraction efficiencies of up to 100% at 0.7 M oxalic acid. At lower acid concentrations, aluminum extraction decreased significantly, with recoveries of approximately 78%, 12%, and 9% for oxalic acid concentrations of 0.5, 0.2, and 0.1 M, respectively (Fig. 9).

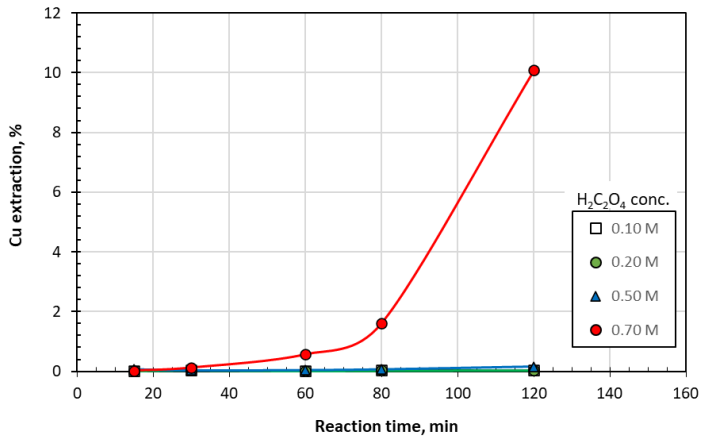

Fig. 8. Cu extraction as a function of time and oxalic acid concentration (T=70°C)

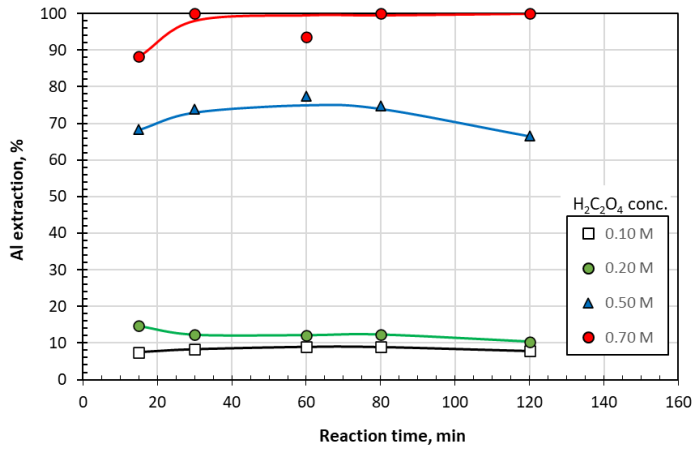

Fig. 9. Al extraction as a function of time and oxalic acid concentration (T=70°C)

Effect of temperature. Leaching experiments were conducted at varying temperatures (50, 70 and 90 °C) while maintaining a constant oxalic acid concentration of 0.5 M. The effects of temperature on the extraction behavior of Li, Fe, Cu, and Al as a function of reaction time are presented in Figures 10–13.

As shown in these figures, increasing the temperature within the tested range had no significant effect on the extraction efficiencies of the target metals. Lithium extraction remained in the range of 75–80%, iron between 3–4%, copper below 0.2%, and aluminum between 70–80%

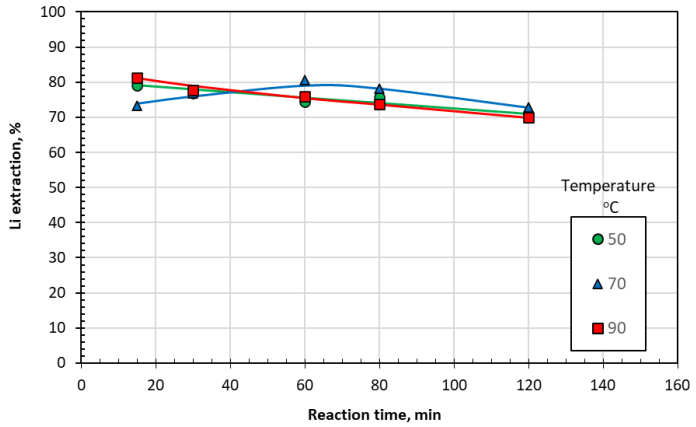

Fig. 10. Li extraction from LFP batteries as a function of time and temperature (0.5 M oxalic acid concentration)

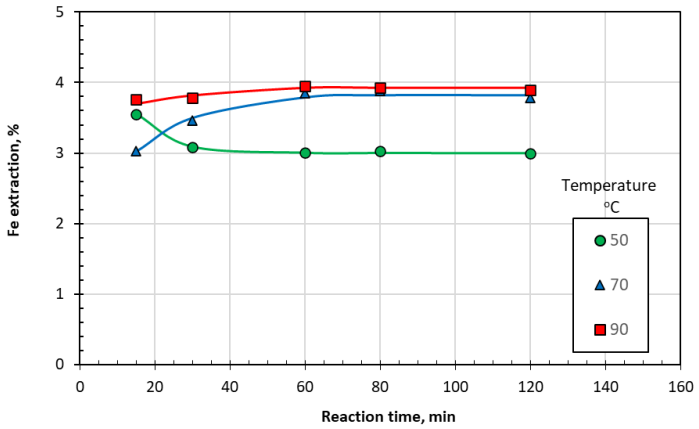

Fig. 11. Fe extraction from LFP batteries as a function of time and temperature (0.5 M oxalic acid concentration)

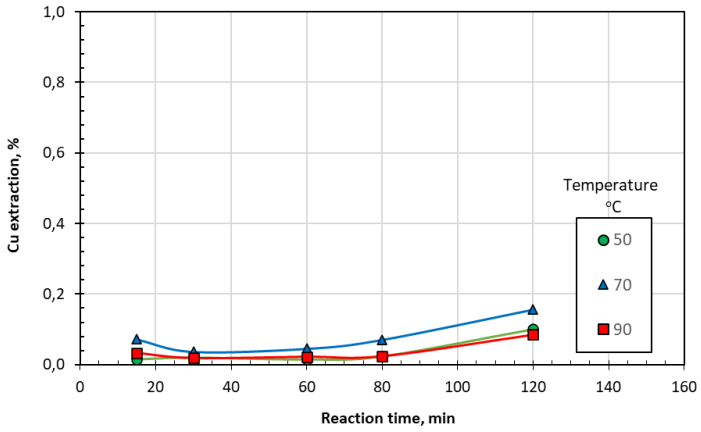

Fig. 12. Cu extraction from LFP batteries as a function of time and temperature (0.5 M oxalic acid concentration)

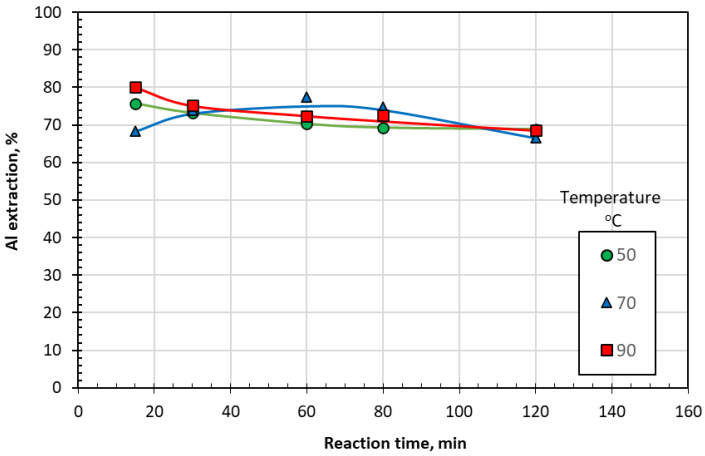

Fig. 13. Al extraction from LFP batteries as a function of time and temperature (0.5 M oxalic acid concentration)

Characterization of leaching solid residues. X-ray diffraction (XRD) analysis patterns performed on the solid leaching residues compared with that of the untreated initial sample, are shown in Fig. 14. As depicted, both the graphite phase and metallic copper remain detectable after leaching. $LiFePO_4$ was identified in residues from leaching conducted under mild conditions (oxalic acid concentrations of 0.1 and 0.2M). In addition, two new crystalline phases, absent in the original material, were identified in the leach residues: humboldtine (hydrated iron oxalate, $FeC_2O_4 \cdot 2H_2O$), which appeared in all residues, and iron phosphate oxide (Fe_3PO_7), which was detected at

oxalic acid concentrations equal or greater than 0.5 M. The presence of these phases was further confirmed by scanning electron microscopy (SEM) analysis.

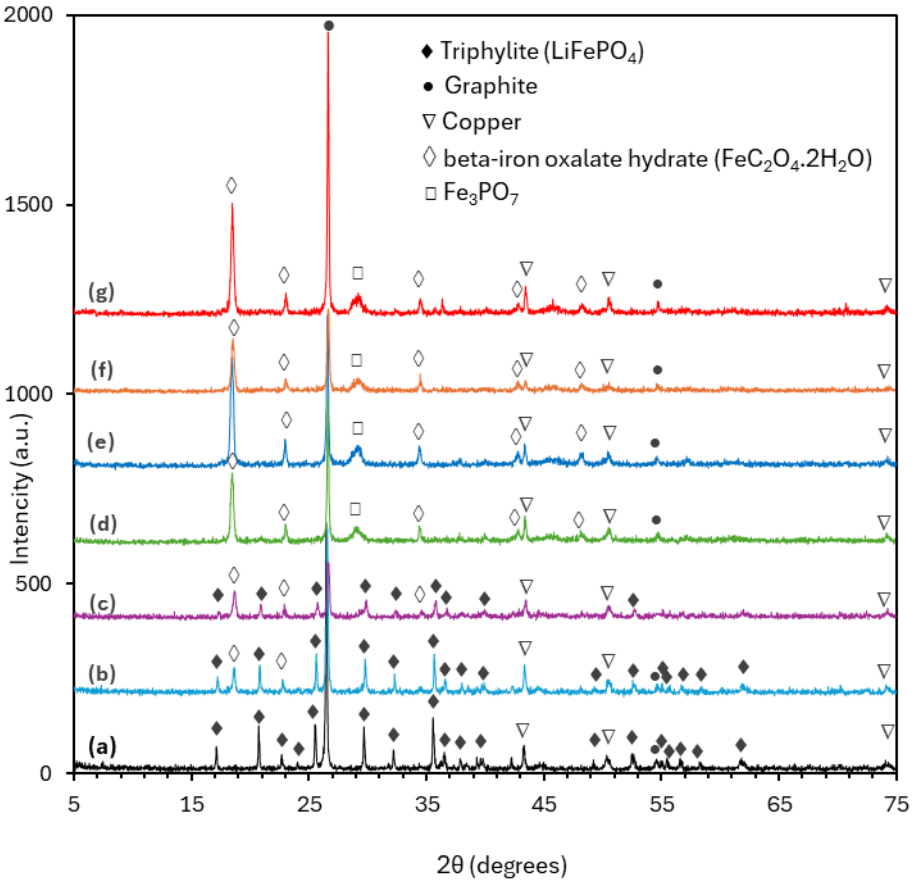

Fig. 14. RD patterns of the initial untreated sample (curve (a)) and solid residues obtained after leaching with oxalic acid under various conditions: curve (b) 0.1 M at 70ºC, (c) 0.2 M at 70ºC, (d) 0.5 M at 70ºC, (e) 0.7 M at 70ºC, (f) 0.5 M at 50ºC, (g) 0.5 M at 70ºC

Conclusions

A comprehensive treatment scheme for end-of-life (EoL) lithium iron phosphate (LFP) batteries was investigated, encompassing both pre-treatment and hydrometallurgical processing. The pre-treatment stage involved initial mechanical shredding and manual removal of the metallic casing, followed by successive crushing, grinding, and sieving steps. These were combined with water-based separation techniques to effectively eliminate plastic, organic, and metallic components. This process yielded a black mass primarily composed of anodic and cathodic active materials, along with residual

metallic impurities, predominantly copper and aluminum originating from the current collectors.

Subsequent leaching experiments conducted using oxalic acid solutions at four concentrations (0.1, 0.2, 0.5, and 0.7 M) under controlled conditions: temperature of 70 °C, liquid-to-solid ratio of 10 l/kg, and reaction times of up to 120 minutes demonstrated complete lithium recovery (≈100%) at an oxalic acid concentration of 0.7 M. At 0.5 M, lithium extraction efficiency ranged from 73% to 80%. Lower concentrations resulted in significantly reduced extraction rates, with 30–35% lithium recovery at 0.2 M and approximately 20% at 0.1 M. Iron dissolution remained consistently low under all leaching conditions and did not correlate with lithium extraction. This behavior is attributed to the precipitation of iron following the dissolution of $LiFePO_4$, primarily in the form of solid iron oxalate and iron phosphate oxide, as confirmed by X-ray diffraction (XRD) analysis of the solid residues. Copper extraction was minimal, with concentrations near the analytical detection limits, except at an oxalic acid concentration of 0.7 M, where extraction increased to approximately 10 percent after 120 minutes, indicating a slight upward trend. Aluminum demonstrated high leachability, with extraction efficiencies reaching up to 100 percent at 0.7 M oxalic acid. At lower concentrations of 0.5, 0.2, and 0.1 M, the extraction efficiencies declined to 78, 12, and 9 percent, respectively. Variations in leaching temperature between 50 °C and 90ºC had no significant impact on the extraction efficiencies of lithium, iron, copper, or aluminum.

The composition of the solid leach residues was strongly dependent on the leaching conditions. At lower oxalic acid concentrations, unreacted components of the starting material, such as $LiFePO_4$, copper, and graphite, remained present in the solid phase. In contrast, higher acid concentrations promoted the formation of secondary iron phases, including hydrated iron oxalate and iron phosphate oxide (Fe_3PO_7), as identified in the XRD patterns, along with residual graphite and copper.

In conclusion, leaching with 0.7 M oxalic acid proved effective for the selective extraction of lithium and its separation from the solid matrix, thereby enabling subsequent recovery from the leachate. Under these conditions, aluminum was co-dissolved to a significant extent, while iron and copper largely remained in the solid phase, limiting their co-dissolution.

References

1. Chen, X., Shen, W., Vo, T.T., Cao, Z., Kapoor, A.: An overview of lithium-ion batteries for electric vehicles. In Proceedings of the 10th International Power & Energy Conference (IPEC), Ho Chi Minh City, Vietnam, 230–235 (2012). https://doi.org/10.1109/ASSCC.2012.6523269
2. Baum, Z.J., Bird, R., Yu, X. and Ma, J.: Lithium-ion battery recycling-overview of techniques and trends. ACS Energy Letters 7(10), 3268-3269 (2022). https://doi.org/10.1021/acsenergylett.2c01888
3. Neumann, J., Petranikova, M., Meeus, M., Gamarra, J.D., Younesi, R., Winter, M., Nowak, S.: Recycling of lithium-ion batteries-current state of the art, circular economy, and next generation recycling. Adv. Energy Mater. 2102917, 1-26 (2022). https://doi.org/10.1002/aenm.202102917

4. Dunn, J.B., Gaines, L., Kelly, J.C., James, C., Gallagher, K.G.: The significance of li-ion batteries in electric vehicle life-cycle energy and emissions and recycling's role in its reduction. Energy Environ. Sci., 8, 158–68. https://doi.org/10.1039/C4EE03029J
5. Takacova, Z., Havlik, T., Kukurugya, F., Orac, D.: Cobalt and lithium recovery from active mass of spent Li-ion batteries: Theoretical and experimental approach. Hydrometallurgy 163, 9–17 (2016). http://dx.doi.org/10.1016/j.hydromet.2016.03.007
6. Lee, C.K. and Rhee, K.-I.: Preparation of LiCoO2 from spent lithium-ion batteries. J Power Sources 109, 17–21 (2002). https://doi.org/10.1016/S0378-7753(02)00037-X
7. Yuliusman, Fajaryanto, R., Nurqomariah, A., Silvia: Acid leaching and kinetics study of cobalt recovery from spent lithium-ion batteries with nitric acid. In 3rd i-TREC 2018, E3S Web of Conferences 67, 03025 (2018). https://doi.org/10.1051/e3sconf/20186703025.
8. Chen, X., Luo, C., Zhang, J., Kong, J., Zhou, T.: Sustainable recovery of metals from spent lithium-ion batteries: A green process. ACS Sustainable Chem. Eng. 3(12), 3104–3113 (2015). https://doi.org/10.1021/acssuschemeng.5b01000.
9. Chen, X., Zhou, T.: Hydrometallurgical process for the recovery of metal values from spent lithium-ion batteries in citric acid media. Waste Manag Res 32(11), 1083-93 (2014). https://doi.org/10.1177/0734242X14557380.
10. Li, L., Bian, Y., Zhang, X., Guan, Y., Fan, E., Wu, F., Chen, R.: Process for recycling mixed-cathode materials from spent lithium-ion batteries and kinetics of leaching. Waste Manag. 71, 362–371 (2018). http://dx.doi.org/10.1016/j.wasman.2017.10.028
11. Gao, W., Song, J., Cao, H., Lin, X., Zhang, X., Zheng, X., Zhang, Y., Sun, Z.: Selective recovery of valuable metals from spent lithium-ion batteries - Process development and kinetics evaluation. J of Cleaner Production 178, 833-845 (2018). https://doi.org/10.1016/j.jclepro.2018.01.040
12. Li, L., Bian, Y., Zhang, X., Yao, Y., Xue, Q., Fan, E., Wu, F., Chen, R.: A green and effective room-temperature recycling process of LiFePO4 cathode materials for lithium-ion batteries. Waste Management 85, 437–444 (2019). https://doi.org/10.1016/j.wasman.2019.01.012
13. Nayaka, G.P., Manjanna, J., Pai, K.V., Vadavi, R., Keny, S.J., Tripathi , V.S.: Recycling of valuable metal ions from the spent lithium-ion battery using aqueous mixture of mild organic acids as alternative to mineral acids. Hydrometallurgy 151, 73–77 (2015). https://doi.org/10.1016/j.hydromet.2014.11.006
14. Zeng, X., Li, J., Singh, N.: Recycling of spent lithium-ion battery: A critical review, Critical Reviews in Environmental Science and Technology, 44(10), 1129–1165 (2014). https://doi.org/10.1080/10643389.2013.763578
15. Meshram, P., Pandey, B.D., Mankhand, T.R.: Extraction of lithium from primary and secondary sources by pre-treatment, leaching and separation: A comprehensive review. Hydrometallurgy 150, 192–208 (2014). http://dx.doi.org/10.1016/j.hydromet.2014.10.012